BIOCHEMISTRY
including biophysical chemistry & molecular biology

Article

pubs.acs.org/biochemistry

R1 Motif Is the Major Actin-Binding Domain of TRIOBP-4

Jianjun Bao,[†] Elizabeth Bielski,[†] Ankita Bachhawat,[†] Doaa Taha,[†] Laura K. Gunther,[†] Kavitha Thirumurugan,[‡] Shin-ichiro Kitajiri,*[,§] and Takeshi Sakamoto*[,†]

[†]Department of Physics and Astronomy, Wayne State University, Detroit, Michigan 48201, United States

[‡]School of Biosciences & Technology, VIT University, Vellore, India

[§]Department of Otolaryngology - Head and Neck Surgery, Graduate School of Medicine Kyoto University, Kyoto, Japan

Supporting Information

ABSTRACT: TRIOBP is an actin-bundling protein. Mutations of *TRIOBP* are associated with human deafness DFNB28. *In vitro*, TRIOBP isoform 4 (TRIOBP-4) forms dense F-actin bundles resembling the inner ear hair cell rootlet structure. Deletion of TRIOBP isoforms 4 and 5 leads to hearing loss in mice due to the absence of stereocilia rootlets. The mechanism of actin bundle formation by TRIOBP is not fully understood. The amino acid sequences of TRIOBP isoforms 4 and 5 contain two repeated motifs, referred to here as R1 and R2. To examine the potential role of R1 and R2 motifs in F-actin binding, we generated TRIOBP-4 mutant proteins deleted for R1 and/or R2, and then assessed their actin-binding activity and bundle formation *in vitro* using actin cosedimentation assays, and fluorescence and electron microscopy. Cellular distributions of the TRIOBP-4 mutants were examined by confocal microscopy. We showed that deletion of both R1 and R2 motifs completely disrupted the actin binding/bundling activities of TRIOBP-4 and impaired its localization to cellular actin cytoskeleton structures. By contrast, TRIOBP-4, lacking only R2 motif, retained its F-actin bundling ability and remained localized to actin filaments in cells, similar to full length TRIOBP-4. On the contrary, the R1 motif-deleted TRIOBP-4 mutant, which mainly consists of the R2 motif, formed thin F-actin bundles *in vitro* but failed to colocalize to actin filaments in cells. These results indicate that R1 motif is the major actin-binding domain of TRIOBP-4, and the binding of R2 motif with actin filaments is nonspecific.

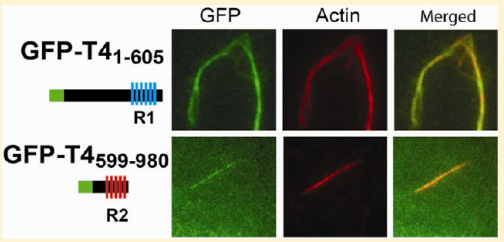

TRIOBP is an actin-bundling protein associated with hearing loss.[1−3] The human and mouse *TRIOBP* genes encode a long isoform and two nonoverlapping short isoforms of TRIOBP proteins, referred to as TRIOBP-5, TRIOBP-4, and TRIOBP-1, respectively. Transcription of TRIOBP-1 (previously named TARA) begins from a downstream open reading frame of TRIOBP-5 and is essential for embryonic development.[2,3] Studies have shown that it binds F-actin directly as well as associates with trio guanine nucleotide exchange factor to regulate actin filament organization[4] and adherens junctions[5] in cells. TRIOBP-4 and -5 are transcribed from the same promoter upstream of TRIOBP-1, but the translation of TRIOBP-4 stops at the end of exon 6 (in human) or exon 8 (in mouse). Thus, there is no sequence in common between TRIOBP-1 and -4. In addition, TRIOBP-1 is ubiquitously expressed, while TRIOBP-4 and -5 are predominantly restricted to the inner ear and the retina.[2,3] In humans, mutations of the *TRIOBP* gene are associated with nonsyndromic deafness DFNB28.[2,3] Surprisingly, all of the mutations identified in human deafness DFNB28 to date are located in exon 6, affecting only *TRIOBP-4/-5*. In mice, joint deletion of *Triobp-4/-5* leads to profound hearing loss without other obvious abnormalities, recapitulating the phenotype seen in human DFNB28 deaf individuals.[1]

Hearing depends on the sound-stimulated deflection of the mechanosensitive organelle known as stereocilia, which are actin-based microvilli-like protrusions on the apical surfaces of inner ear hair cells. The core of stereocilia contains parallel actin filaments that are cross-linked into bundles by F-actin interacting proteins including espin, fimbrin, and fascin.[6−12] At the base of stereocilia, the actin filaments are organized into even denser structures called rootlets extending into the hair cell body.[13] We have previously reported that TRIOBP is an actin-bundling protein localized at the rootlets and is responsible for the dense actin bundle formation of the rootlets.[1] *In vitro*, purified TRIOBP-4 protein packs actin filaments into dense bundles resembling the *in vivo* structure of rootlets. The stereocilia of *Triobp-4/-5* deficient mice failed to form rootlets, which is considered to be the primary cause of hearing loss in these mice. Unlike espin 3A, an actin cross-linker in the core of stereocilia which intercalates between actin filaments to generate interfilaments spaces, TRIOBP-4 forms much more condensed F-actin bundles, and no interfilament space is detected.[1] How TRIOBP-4 forms such dense F-actin bundles is unknown. Nevertheless, this unique bundle feature implies that the manner in which TRIOBP-4 regulates actin bundle organization is different from other previously studied actin-bundling proteins, including espins.

Received: October 16, 2012
Revised: June 18, 2013
Published: June 21, 2013

   dx.doi.org/10.1021/bi400585h | *Biochemistry* 2013, 52, 5256−5264

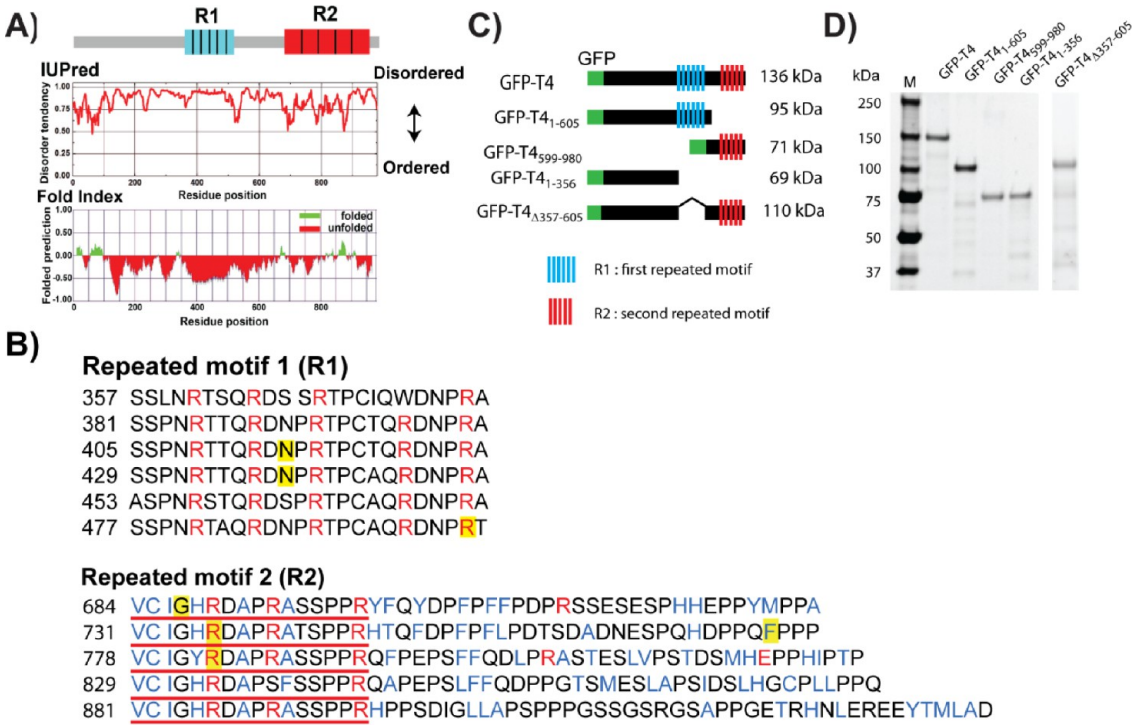

Figure 1. Structural analysis of TRIOBP-4 and generation of TRIOBP-4 truncated proteins. (A) Protein disorder prediction by IUPred and FoldIndex. (B) Amino acid sequences of repeated motif 1 (R1) and motif 2 (R2). The underlines indicate the repeated amino acid sequence in R2 motif. (C) Diagram of GFP-TRIOBP-4 protein (GFP-T4) and its mutants lacking R2 motif (GFP-T4$_{1-605}$), or R1 motif (GFP-T4$_{599-980}$ and GFP-T4$_{\Delta357-605}$), or both motifs (GFP-T4$_{1-356}$). (D) Representative SDS-PAGE of purified TRIOBP-4 full-length and truncated proteins. M, protein molecular weight markers.

Since TRIOBP is important for hearing, understanding the mechanism of F-actin bundling by TRIOBP-4 would provide us essential information on human deafness DFNB28. As the first step to investigate its F-actin bundling mechanism, we focused on the exon 6 region of human *TRIOBP-4/-5*, where mutations are associated with hearing loss. Exon 6 of *TRIOBP-4/-5* encodes several copies of two repeated motifs called R1 and R2.[1] They are of particular interest, for among the 13 deafness-causing point mutations identified, six nonsense mutations leading to a premature stop of translation are found in R1 and R2 motifs.[1] Moreover, an additional missense mutation encoding a mutant TRIOBP is also located in the R2 motif. Mouse *Triobp-4* has a similar structure to human *TRIOBP-4* including the repeated motifs in exon 8, which is equivalent in DNA sequence to exon 6 in humans. Despite the importance of these motifs in hearing, their molecular and cellular functions have not been revealed yet. Here, using microscopy methods and biochemical analyses, we studied F-actin bundle formation with TRIOBP-4 truncated proteins that are deleted for the R2 or/and R1 motifs. We provided evidence that the R1 motif is the major actin-binding domain responsible for F-actin bundle formation.

EXPERIMENTAL PROCEDURES

***Triobp-4* Constructs.** The constructs encoding mouse TRIOBP-4-FLAG and GFP-TRIOBP-4-FLAG in pFast-Bac1 vector were described previously.[1] cDNAs encoding truncated proteins corresponding to the amino acid sequences 1−605, 1−356, and 599−980 of mouse TRIOBP-4, or mutant TRIOBP-4 lacking the amino acids 357−605 (see Figure 1B) with or without a GFP-tag to their N-terminus were amplified by PCR and subcloned into SpeI/NotI sites of pFast-Bac1 vector containing a FLAG tag (DYKDDDDK)[14] at the C-terminus for baculovirus-Sf9 cell expression system. The GenBank number (accession number) for TRIOBP-4 sequences reported in this paper is DQ228002. For mammalian expression, mutant *Triobp-4* PCR products were inserted into *Hin*dIII/*Sal*I sites of pAc-GFP1 vector (Clontech). All of the constructs were verified by DNA sequencing analysis.

RNA Purification and RT-PCR. Total RNA from cultured cells were extracted using RNeasy kit (Qiagen), and the first strand cDNA was synthesized using Superscript III reverse transcriptase and random hexamers as primers (Life Technologies). Two microliters of 20 μL cDNA reaction mixtures was used for PCR. The primers for human *TRIOBP-1* (accession number: NM007032) and *TRIOBP-3/-5* (accession numbers: DQ278603, DQ228003, and DQ228005) were described previously.[3] The primers for human *TRIOBP-4* (accession number: DQ228004) were forward, 5′-CTCTTC-GCCCCCTCGCTATT-3′; reverse, 5′- CTTCACCTGTCC-TGCTGCCGA-3′. The reverse primer of *TRIOBP-4* is targeted to its 3′ UTR region.

Protein Preparation. The full-length and mutant *Triobp-4* constructs in pFast-Bac1 vector were used to generate recombinant baculoviruses in Sf9 insect cells for protein expression.[1] The proteins were purified from Sf9 cell lysates using FLAG affinity chromatography followed by a gel filtration column as described.[1] Purified proteins were stored in the buffer containing 10 mM MOPS, pH 7.4, 100 mM KCl, 0.1 mM EGTA, and 2 mM $MgCl_2$, and their concentrations were determined by using the extinction coefficients ($A_{280}-A_{320}$) calculated from their cDNA sequences. The purity of each protein preparation was examined by SDS-PAGE. Actin was purified from rabbit skeletal muscle[15] and was stored as G-actin

dx.doi.org/10.1021/bi400585h | *Biochemistry* 2013, 52, 5256−5264

in G-buffer (0.2 mM ATP, 1 mM NaN_3, 0.2 mM $CaCl_2$, 0.5 mM DTT, and 2 mM Tris-HCl, pH 8.0).

High- and Low-Speed F-Actin Cosedimentation Assays. G-Actin was polymerized by addition of 100 mM KCl, 5 mM $MgCl_2$, and 1 mM ATP into G-buffer for 2 h at room temperature or overnight on ice. Indicated amounts of purified TRIOBP-4 proteins were incubated with 8 μM of F-actin for 1 h in the presence of 100 mM or 10 mM KCl, and the reaction mixtures were centrifuged at 385000*g*, 15 min for high-speed cosedimentation assay and 11000*g*, 15 min for low-speed cosedimentation assay. All the above procedures were performed at 23 °C. Equal volumes of supernatants and pellets from the assays were analyzed by 4−20% SDS-PAGE. The density of each protein band was measured by densitometry (Gel-Doc, EZ, Bio-Rad) and normalized to TRIOBP-4 protein alone. The actin-binding activity of each TRIOBP-4 protein was quantified as described.[1]

Fluorescence Microscopy. The fluorescence microscope was set up with an inverted microscope (IX81, OLYMPUS). Three diode pumped lasers (473 nm, 556 nm, and 655 nm wavelength; OEM Laser, MI) were introduced from the right side port of a cube turret into the IX81. Each laser was individually focused by a biconvex lens at the back focal plane of objective lenses (x60, N.A.:1.49, APON, OLYMPUS) and set up in a total internal reflection fluorescence (TIRF) mode, which increases the signal-to-noise ratio. F-actin was fluorescently labeled with rhodamine-phalloidin using a standard method.[16] GFP-TRIOBP-4 proteins were incubated with rhodamine-phalloidin-labeled F-actin at 1:10 (2 μM TRIOBP: 20 μM F-actin), 1:1 (2 μM TRIOBP: 2 μM F-actin), and 10:1 (10 μM TRIOBP: 1 μM F-actin) ratios in the presence of 10 or 100 mM KCl and applied to a flow cell as described[17] followed by epifluorescence microscopy. Images were acquired by an EMCCD camera (ImagEM, model: C9100−13, Hamamatsu photonics USA) through relay lenses (x2 and x4). The fluorescence intensity of F-actin bundles was analyzed by using MetaMorph (Molecular Devices). The data were normalized to the intensity of a single actin filament.

Transmission Electron Microscopy (TEM). For EM imaging, G-actin was polymerized as described above. F-actin bundles were prepared by incubating TRIOBP-4 proteins with F-actin at 1:10 (2 μM TRIOBP: 20 μM F-actin), 1:1 (2 μM TRIOBP: 2 μM F-actin), and 10:1 (20 μM TRIOBP: 2 μM F-actin) ratios in the presence of 10 or 100 mM KCl for 1 h at room temperature. The protein samples (total protein 0.2−4 mg/mL) were applied to 400-mesh Formvar carbon grids (FCF400-Cu, Electron Microscopy Sciences), absorbed onto the grids for 30s, washed with 1× PBS buffer, and negatively stained with 1% aqueous uranyl acetate for 1 min. The images of a F-actin bundle with TRIOBP-4 or its mutants were taken using transmission electron microscope (TEM, JEOL-2010) at 100 keV and various magnifications as described.[1,18]

Cell Culture, Transfection, and Confocal Fluorescence Microscopy. HEK293, HepG2, HPAC, and HeLa cell lines were obtained from ATCC and cultured in media supplemented with 10% fetal bovine serum (Life Technologies). pAcGFP1-TRIOBP-4 (GFP-T4) or its mutant constructs were transfected into HeLa cells using lipofectamine 2000 (Life Technologies) according to the manual. Eighteen hours after transfection, cells were fixed with 4% paraformaldehyde for 15 min, followed by incubation with 0.1% Triton X-100 for 10 min. Actin filaments were stained with Alexa Fluor 633-labeled phalloidin (1:40 dilution) for 20 min. The stained cells were mounted with ProLong Gold Antifade Reagent (Life Technologies). All the procedures were performed at room temperature. Confocal images were taken using a Leica microscope (model: Leica TCS SP5).

RESULTS

Structural Analysis of TRIOBP-4 and Generation of Mutant TRIOBP-4 Proteins. As a first step to identify the actin-binding sites in TRIOBP-4, we applied web-based software Phyre2[19] to predict the secondary structure of TRIOBP-4. In the sequence, 99% of the amino acid residues were predicted to be disordered. We further analyzed the sequence using IUPred[20] and FoldIndex.[21] Both programs predict that TRIOBP-4 is an unfolded protein (Figure 1A). Since there is no information regarding its secondary structure, we decided to investigate the R1 and R2 motifs, because their primary sequences contain several copies of characteristic repeats (Figure 1B,C) and are the targets for hearing loss mutations in humans. The R1 motif contains six copies of a 24-amino acid repeat, while the R2 motif consists of five copies of a shorter repeat with 16-amino acids (Figure 1B, red underscore) in a 50-amino acid interval. These two motifs are enriched in residues arginine (20.1% in R1), serine (11.9% in R1 and 12.4% in R2), and proline (14.9% in R1 and 22.4% in R2), which is the characteristic of a disordered protein (Figure 1B).[22] Although R1 and R2 motifs are predicted to have highly disordered structure (Figure 1A), the calculated pI values between R1 and R2 motif are different, 11.7 and 5.4, respectively. This may affect the binding activity of TRIOBP-4 to F-actin.

As such, we generated truncated mouse TRIOBP-4 (T4) proteins missing either R2 ($T4_{1-605}$), or R1 ($T4_{\Delta357-605}$), both R1 and R2 ($T4_{1-356}$), as well as the fragment majorly composed by R2 ($T4_{599-980}$) using the baculovirus expression system in Sf9 insect cells (Figure 1C). GFP was fused to the N-terminus of these proteins, and a FLAG tag was introduced at their C-terminus. We confirmed the purity of the expressed proteins by SDS-PAGE (Figure 1D) and examined their actin-binding and bundling activities by sedimentation assays described below. The molecular weights of GFP-T4 proteins were higher on SDS-PAGE than expected (Figure 1D). We interpret that this was caused by the high content of proline residues in these fragments (see Discussion).

Actin-Binding Activities of TRIOBP-4 Mutants. The F-actin binding affinity of TRIOBP-4 was examined by high-speed cosedimentation assay with increasing amounts of TRIOBP-4 proteins and a constant concentration of F-actin (8 μM) at 100 mM KCl, followed by SDS-PAGE analysis. None of the truncated fragments of TRIOBP-4 sediment in the absence of F-actin, confirming that the GFP-T4 fragments were not aggregated (Supplemental Figure S1, Supporting Information). Some degradation fragments were seen in the SDS-PAGE (Figure 2A−E). The GFP-T4 proteins, except for GFP-$T4_{1-356}$, pelleted with F-actin in a dose-dependent manner, while most of the GFP-$T4_{1-356}$ protein was detected in the supernatant fraction, and very little pelleted with F-actin (Figure 2A−D). The pelleted GFP-$T4_{1-356}$ may be caused by nonspecific trapping of excess F-actin. Strikingly, the R1-containing fragment GFP-$T4_{1-605}$ showed much higher saturated binding activity than the intact GFP-T4, and the stoichiometry between GFP-$T4_{1-605}$ and actin was 2-fold higher than that of intact GFP-T4 and actin (1.2 ± 0.11 vs 0.39 ± 0.1). On the other hand, the ratio between TRIOBP-4 and actin of the R2-

dx.doi.org/10.1021/bi400585h | *Biochemistry* 2013, 52, 5256−5264

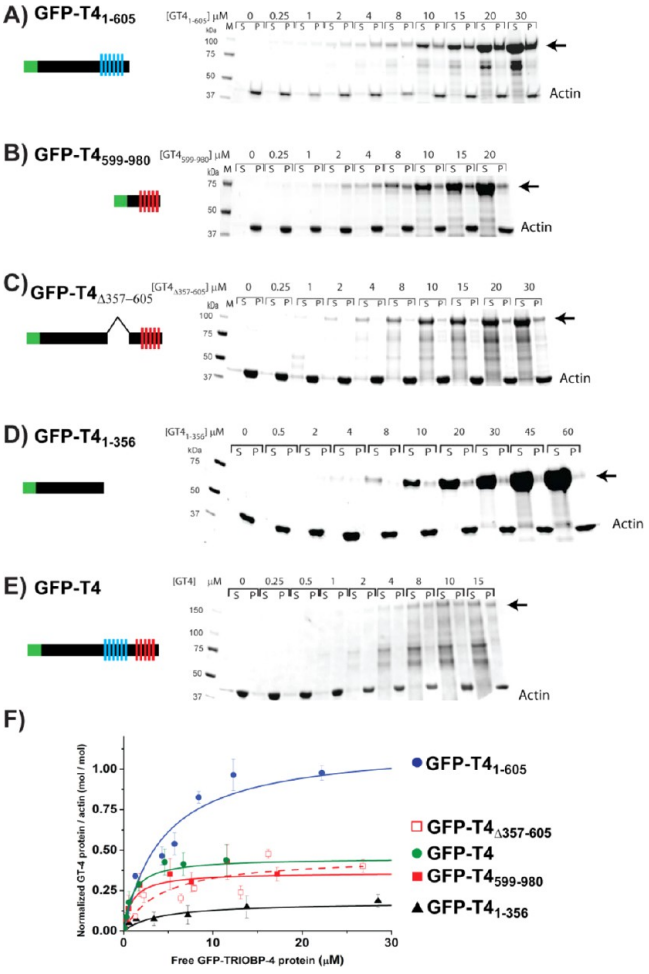

Figure 2. High-speed F-actin cosedimentation assays of full-length and mutant TRIOBP-4 proteins. (A–E) Representative Coomassie blue staining images of SDS-PAGE from high speed cosedimentation assay of GFP-T4$_{1-605}$ (A), GFP-T4$_{599-980}$ (B), GFP-T4$_{\Delta357-605}$ (C), GFP-T4$_{1-356}$ (D), and GFP-T4 (E) in the presence of 100 mM KCl. S, Supernatant; P, pellet. Arrows represent the intact TRIOBP-4 proteins. (F) Quantitative analyses of actin-binding activities obtained from high-speed cosedimentation. Data were fit by hyperbolic function and represent means ± standard deviation from at least four independent experiments.

containing fragments GFP-T4$_{599-980}$ and GFP-T4$_{\Delta357-605}$ were close to that of GFP-T4. By contrast, the GFP-T4$_{1-356}$ fragment lacking both R1 and R2 motifs showed little F-actin binding activity with a low F-actin binding ratio of 0.18 (Figure 2F and Table 1). The dissociation constant (K_d) of GFP-T4$_{1-605}$ for F-actin (2.9 ± 0.31 μM) is higher than that of GFP-T4 (0.91 ± 0.22, Figure 2F and Table 1). The actin-binding activity is very different between the two R2 containing fragments. The K_d of GFP-T4$_{599-980}$ (0.98 ± 0.23 μM) is similar to that of GFP-T4, while the K_d of GFP-T4$_{\Delta357-605}$ (4.21 ± 0.83 μM) is much higher than that of GFP-T4 (Figure 2F and Table 1).

We also performed high-speed assay in an alternative way, that is, using fixed amount of GFP-TRIOBP-4 or TRIOBP-4 fragments in the presence and the absence of a GFP tag and increasing concentrations of F-actin with different ionic strengths (Supplemental Figures S1 and 2). Consistent with the results of Figure 2, at 100 mM KCl, most of GFP-T4$_{1-356}$ protein did not pellet with F-actin. The K_d's of GFP-T4$_{1-605}$ and T4$_{1-605}$ were similar at 2.46 ± 0.22 μM and 2.41 ± 0.26 μM, respectively. The saturation of GFP-TRIOBP-4$_{1-605}$ (0.98) is also similar to that of T4$_{1-605}$ (0.82, Supplemental Figures 1C and 2C). The R2-containing fragments (GFP-T4$_{599-980}$, T4$_{599-980}$, and GFP-T4$_{\Delta357-605}$) showed about 50% saturation. However, their K_ds greatly varied. The K_ds of T4$_{599-980}$ (6.36 ± 0.47 μM) and GFP-T4$_{\Delta357-605}$ (4.85 ± 0.12 μM) are much higher than that of GFP-T4$_{599-980}$ (1.25 ± 0.09 μM) (Supplemental Figure S1, Supplemental Figure S2, and Supplemental Table 1). Furthermore, decreasing the ionic strength to 10 mM KCl significantly increased the actin-binding activity of GFP-T4$_{1-605}$ and T4$_{1-605}$ (K_d: 0.52 ± 0.15 μM and 0.56 ± 0.10 μM, respectively) but not GFP-T4$_{599-980}$ and T4$_{599-980}$ (K_d: 1.29 ± 0.12 μM and 4.55 ± 0.38 μM, respectively, Supplemental Figure S1, and Supplemental Table 1), indicating that the R2 motif interacting with F-actin is likely hydrophobic.

F-Actin-Bundling Activities of TRIOBP-4 Mutants. Unlike unbundled F-actin, which requires high centrifugal forces for sedimentation, actin bundles sediment at low centrifugal speeds. We next performed low-speed F-actin cosedimentation assay to assess the F-actin bundling activity of the above TRIOBP-4 fragments using variable amounts of TRIOBP-4 proteins and a constant concentration of F-actin. Similar to actin binding experiments above (Figure 2), very little F-actin was pelleted in the presence of the TRIOBP-4 fragment GFP-T4$_{1-356}$ even when higher concentrations of GFP-T4$_{1-356}$ were used (Figure 3D). More F-actin was pelleted in the presence of the R1 motif-containing fragment GFP-T4$_{1-605}$ than in the presence of the R2 motif-containing fragments GFP-T4$_{599-980}$ and GFP-T4$_{\Delta357-605}$ (Figure 3A–C,E). Interestingly, the majority of the F-actin pelleted by 2 μM GFP-T4$_{1-605}$ (Figure 3A), meaning that most of the actin was bundled by the R1 motif at low ratios of fragment: actin. Additional TRIOBP-4$_{1-605}$ protein could be added to the bundle as the concentration was increased. This result suggests that R1 motif may have a different mechanism of F-actin bundling (see Discussion). In addition, GFP did not affect the actin bundling activity of both GFP-T4$_{1-605}$ and GFP-T4$_{599-980}$ (Figure 3E and Supplemental Figure S3C). Taken together, the high and low-speed F-actin cosedimentation assays indicate that the amino acid sequence 357–598 of TRIOBP-4, which is mainly composed of R1 motif, is the major domain responsible for TRIOBP-4's F-actin binding and bundling activities.

Table 1. Dissociation Constant and the Stoichiometry from High- and Low-Speed Co-Sedimentation Assays

	GFP-T4	GFP-T4$_{1-605}$	GFP-T4$_{599-980}$	GFP-T4$_{357-605}$
dissociation constant (K_d, μM)	0.91 ± 0.22	2.91 ± 031	0.98 ± 0.23	4.21 ± 0.83
stoichiometry (high-speed cosedimentation)	0.39 ± 0.10	1.20 ± 0.11	0.33 ± 0.07	0.46 ± 0.09
stoichiometry (low-speed cosedimentation)	0.29 ± 0.01[a]	1.10 ± 0.18	0.26 ± 0.13	0.41 ± 0.09

[a]Data are Figure 3C in Kitajiri, S., et al., 2010, *Cell*, **141**, 786.

dx.doi.org/10.1021/bi400585h | *Biochemistry* 2013, 52, 5256–5264

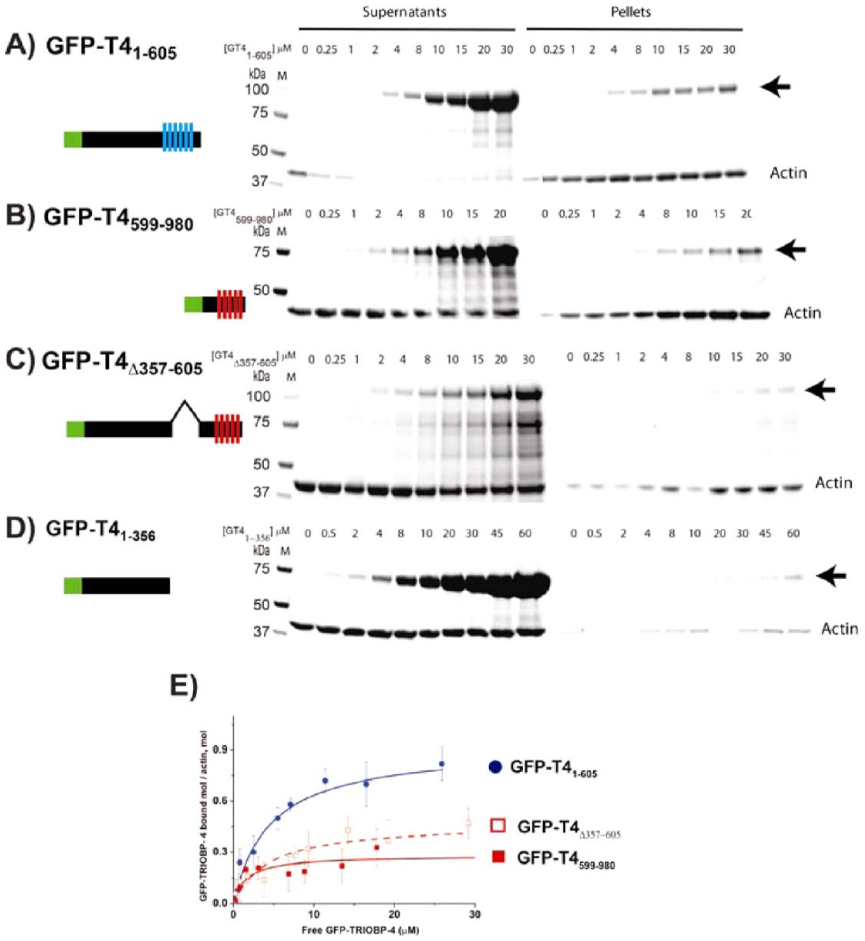

Figure 3. Low-speed F-actin cosedimentation assays of GFP-TRIOBP-4 mutant proteins. (A–D) Representative Coomassie blue staining images of SDS-PAGE from low speed cosedimentation assay of GFP-T4$_{1-605}$ (A), GFP-T4$_{599-980}$ (B), GFP-T4$_{\Delta357-605}$ (C), and GFP-T4$_{1-356}$ (D). Arrows represent the position of TRIOBP-4 proteins. (E) Quantitative analysis of actin-bundling activities of low speed cosedimentation assays of GFP-T4$_{1-605}$ (blue circle), GFP-T4$_{599-980}$ (red closed circle), and GFP-T4$_{\Delta357-605}$ (red open circle). Data were fit with hyperbolic function.

GFP-T4$_{599-980}$ and GFP-T4$_{1-605}$ Do Not Functionally Interact. GFP-T4$_{1-605}$ binds somewhat more weakly to F-actin and with a high stoichiometry than does full-length TRIOBP-4 (Table 1 and Supplemental Table 1). To test the possibility that the GFP-T4$_{599-980}$ fragment may have a regulatory role in the F-actin binding activity of GFP-T4$_{1-605}$ *in vitro*, we performed "co-binding" experiments to see whether the presence of GFP-T4$_{599-980}$ would inhibit the binding of GFP-T4$_{1-605}$ to F-actin. Briefly, 10 μM GFP-T4$_{1-605}$ and 8 μM F-actin were mixed with various concentrations of GFP-T4$_{599-980}$, followed by high-speed F-actin cosedimentation assays. As seen in Supplemental Figure S4A, the binding activity of GFP-T4$_{1-605}$ to F-actin was not significantly changed by the increased amounts of GFP-T4$_{599-980}$. Therefore, these results do not support a direct interaction of the two fragments for modulating the binding of GFP-T4$_{1-605}$ to F-actin under our current *in vitro* conditions. We also performed low-speed F-actin cosedimentation assay for the "co-binding" experiment as described above. Similar to the high-speed assay, the F-actin bundling activity of GFP-T4$_{1-605}$ was not significantly changed by the increased concentrations of GFP-T4$_{599-980}$, either (Supplemental Figure 4SB). The K_d of GFP-T4$_{599-980}$ is higher in "co-binding" experiment than in GFP-T4$_{599-980}$ alone experiment (5.4 μM vs 0.98 μM), presumably resulting from the less free binding sites for GFP-T4$_{599-980}$ in the presence of GFP-T4$_{1-605}$.

R1 is the Major Actin-Binding Domain of TRIOBP-4 for F-Actin Bundle Formation in Vitro. We next directly visualized F-actin bundle formation by GFP-T4$_{1-605}$ and GFP-T4$_{599-980}$ under the same conditions as the low-speed cosedimentation assays. First, we imaged actin filaments bundled with GFP-T4$_{1-605}$ and GFP-T4$_{599-980}$ using fluorescence microscopy. Truncated GFP-T4 proteins were incubated with rhodamine-phalloidin-labeled actin filaments in a molar ratio of 1:1, and the binding of GFP-T4 proteins (green) with F-actin (red) were observed under an epi-fluorescence microscope (Figure 4A). In the presence of 10 mM KCl, GFP- T4$_{1-605}$ formed thick F-actin bundles containing about 10 actin filaments in a bundle (Figure 4A, left middle panels and 4B). Similar to the biochemical assays, the size of the GFP-T4$_{1-605}$-F-actin bundles was influenced by ionic strength. When adding KCl to a final concentration of 100 mM to the GFP-T4$_{1-605}$-F-actin mixture, the number of actin filaments decreased to about five in a bundle (Figure 4A, left bottom panels, and 4B), and some of the F-actin disassociated from the preformed bundles (Figure 4A, yellow square 1, which is enlarged in Figure 4C, 1). By contrast, GFP-T4$_{599-980}$ formed needle-like, thin F-actin bundles whose structures were not affected by increasing the KCl concentration to 100 mM (Figure 4A, right middle and bottom panels). The GFP-T4$_{599-980}$-F-actin bundle contained about five actin filaments under both high and low KCl conditions (Figure 4B), and no

dx.doi.org/10.1021/bi400585h | *Biochemistry* 2013, 52, 5256–5264

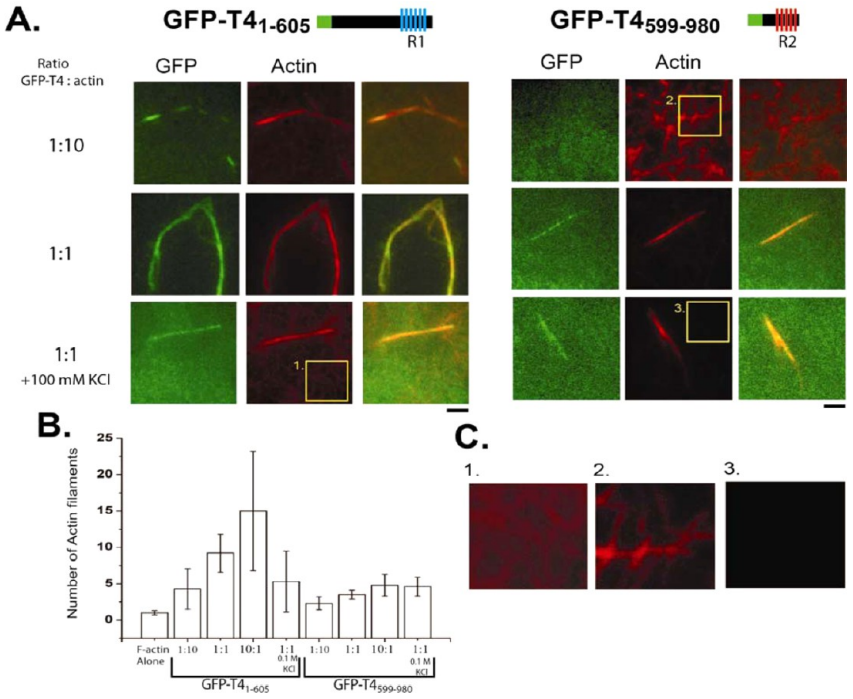

Figure 4. Fluorescence microscopy analysis of F-actin bundle formation with GFP-TRIOBP-4 mutants. (A) Fluorescence images of rhodamine-phalloidin-labeled F-actin bundles (red) with GFP-T4$_{1-605}$ (left panels) and GFP-T4$_{599-980}$ (right panels) in a ratio to F-actin at 1:10 and 1:1 in the presence of 10 mM KCl (top and middle rows) or 1:1 in the presence of 100 mM KCl (bottom rows). Scale bar: 200 nm. (B) Quantitative analysis of actin filament numbers within a bundle. The signal intensity of rhodamine-phalloidin labeled F-actin bundles was measured in a rectangle region of interest (200 × 500 μm, n = 30−40) and was normalized to the intensity of single actin filament. Data represent means ± standard deviation. (C) Enlarged images of the insets shown in A.

obvious F-actin disassociation was observed under 100 mM KCl (Figure 4A yellow square 3, which is enlarged in Figure 4C, 3). We also examined the actin bundle formation with TRIOBP-4 mutants by changing the protein/actin ratio at 10 mM KCl. When the TRIOBP protein to F-actin ratio was decreased to 1:10, GFP-T4$_{1-605}$ was still able to form thin F-actin bundles (Figure 4A, left top panels), whereas GFP-T4$_{599-980}$ lost F-actin bundling activity (Figure 4A, top panels, yellow square 2 is enlarged in Figure 3C, 2).

F-actin bundle formation with GFP-T4 mutants were also examined by electron microscopy (Figure 5). Consistent with those obtained from fluorescence microscopy (Figure 4), TEM imaging also revealed that GFP-T4$_{1-605}$ formed much thicker F-actin bundles than did GFP-T4$_{599-980}$ when protein to actin ratio was 1:1 and 10:1 in the presence of 10 mM KCl. Similarly, at lower protein to actin ratio (1:10), GFP-T4$_{1-605}$ bundles actin filaments, while GFP-T4$_{599-980}$ was unable to do so.

Together with the biochemical assays, the microscopy results indicate the R1 motif is responsible for F-actin bundle formation. The thin F-actin bundle formed by GFP-T4$_{599-980}$, which contains R2 motif (amino acids 684−939), is most likely caused by the nonspecific binding to actin (see Discussion).

R1 Motif but not R2 Motif Is Essential for Actin Cytoskeleton Localization in Cells. To verify our results obtained *in vitro*, we examined the cellular distribution of TRIOBP-4 mutant proteins with respect to actin cytoskeleton structure. RT-PCR revealed that TRIOBP-4 is expressed in several human cell lines, including HeLa cells, which do not express the long isoform TRIOBP (Figure 6A). We transiently overexpressed GFP-TRIOBP-4 full-length (GFP-T4) and its three mutants, GFP-T4$_{1-605}$, GFP-T4$_{1-356}$, and GFP-T4$_{599-980}$ in HeLa cells and observed their colocalization with actin

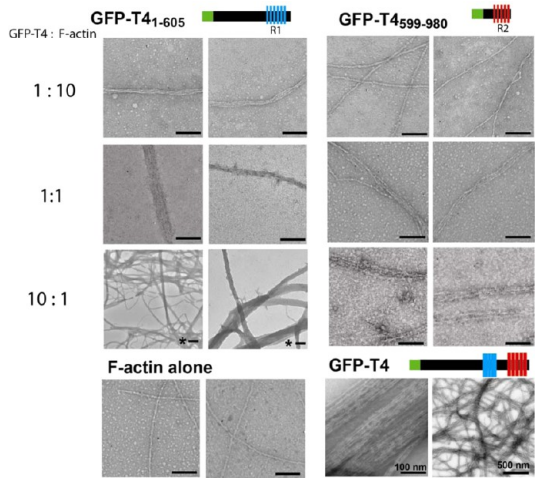

Figure 5. Transmission electron microscopy images of F-actin bundles with full-length and mutant GFP-TRIOBP-4. Representative images of F-actin bundle structures formed by GFP-TRIOBP-4 mutants in the presence of 10 mM KCl. Three different ratios between TRIOBP-4 fragment and F-actin are shown. F-actin alone and full-length GFP-T4 images were shown at the bottom as controls. Scale bar, 100 nm, except for the 10:1 ratio of GFP-T4$_{1-605}$-F-actin bundle as asterisk is 300 nm.

filaments by confocal microscopy. Cells with the lowest expression level of TRIOBP-4 and intact actin filaments were chosen for analysis. Both the GFP-T4 full-length and GFP-T4$_{1-605}$ are shown to localize in actin cytoskeleton structure including filopodia, where parallel actin bundles are formed (Figure 6B). In contrast, GFP-T4$_{1-356}$ and GFP-T4$_{599-980}$ are

dx.doi.org/10.1021/bi400585h | *Biochemistry* 2013, 52, 5256−5264

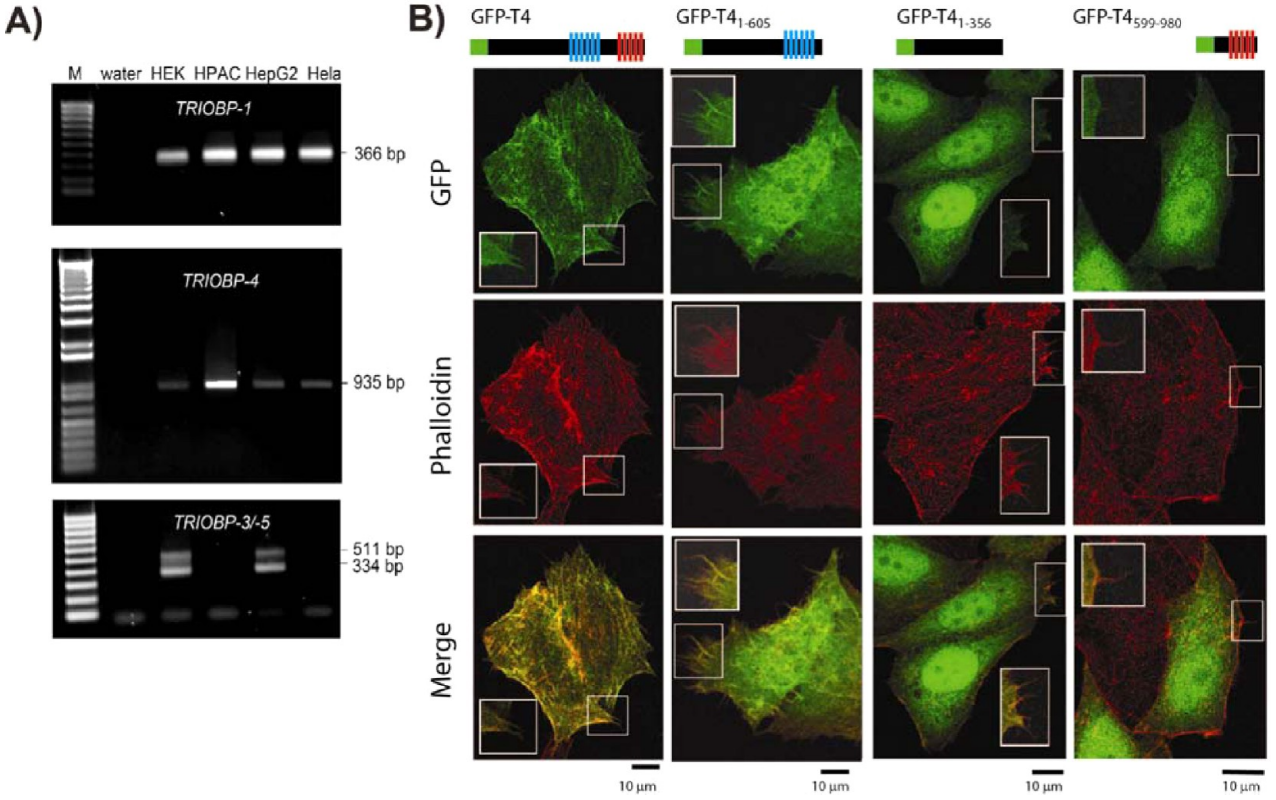

Figure 6. *TRIOBP* mRNA expression and colocalization of TRIOBP-4 and its mutants with F-actin in cells. (A) RT-PCR analysis of *TRIOBP* isoforms in several human cell lines. The expected sizes of PCR products were indicated. (B) HeLa cells overexpressing GFP-T4 and its three mutants (green) were stained with Alexa Fluor 633-labeled phalloidin (red) to visualize F-actin. Merged images of GFP and Alexa Fluor 633 were shown in the bottom rows. Scale bar, 10 μm.

uniformly expressed within the cytoplasm of the cells, showing no specific localization to F-actin (Figure 6B). Thus, consistent with our *in vitro* observations of actin bundle formation described in Figures 4 and 5, these results indicate that the R1 motif of TRIOBP-4 is the major domain for actin filament assembly in cells, while the R2 motif alone was unable to form detectable filamentous structures in cells.

DISCUSSION

Collectively, our results demonstrate that the R1 motif is the major F-actin binding domain of TRIOBP-4, an actin-bundling protein mutated in human deafness DFNB28. Through deletion mutagenesis, we show that the R1 motif is crucial for the binding activity and F-actin bundle formation of TRIOBP-4, as well as its proper cytoskeleton localization in cells.

In general, actin-bundling proteins contain at least two actin-binding sites per monomer or exist as a dimer or higher oligomer, and are intercalated between actin filaments to form hexagonally packed bundles.[23−27] For example, fimbrin, espin 3A, and fascin are monomeric and contain two actin-binding sites.[28−31] In contrast, α-actinin and spectrin are dimers, and each peptide chain has one actin-binding site.[27,32,33] In both cases, interfilament spaces in an F-actin bundle are generated, which are affected by the space between the two actin-binding sites. However, the bundles formed by TRIOBP-4 could not be explained by an "intercalation" model because they lack obvious interfilament spaces.[1] Previously, we proposed that TRIOBP-4 "wraps around" the surfaces of actin filaments so that filaments are aligned closely enough without any spaces within a bundle. Our current studies strongly support this model. First, structural analyses predict that TRIOBP-4 is an unfolded, disordered protein without any known secondary structures (Figure 1A). Moreover, EM images did not show any globular structures of TRIOBP-4 or its mutants between filaments in the bundle (Figure 5), further supporting the prediction. This structural property of TRIOBP-4 makes it possible to function as an unfolded "string" which flexibly "wraps around" the filaments through its actin-interacting domain located in the R1 motif. Second, F-actin binding/bundling activities and bundle formation by the R1 motif are regulated by ionic strength (Figure 4 and Supplemental Figures S1 and S2), suggesting that binding of the R1 motif to F-actin is more likely to be an electrostatic interaction mediated by a certain region of R1 rather than specific binding sites as found in other actin bundling proteins such as espin 3A and fascin. In this regard, it is interesting that the pI of the R1 motif (11.7) is much higher than that of actin (pI 4.8), which could lead to strong electrostatic interaction under the assay condition (pH 7.4). Third, the affinity of TRIOBP-4 for F-actin is much weaker than that of espin3A as evidenced by a F-actin dissociation constant K_d of 0.9 μM for TRIOBP-4 compared to 0.15 μM for espin.[1,29] This may reflect a nonspecific "wrapping" type of binding through electrostatic interactions that is not as strong as an intercalated cross-linker between filaments through specific binding sites. Finally, our low-speed sedimentation assay demonstrated that though most of the F-actin bundles were formed at low ratios of GFP-T4$_{1-605}$ to actin, additional GFP-T4$_{1-605}$ was still able to bind actin when GFP-T4$_{1-605}$ was further increased, indicating that binding of the R1 motif with

dx.doi.org/10.1021/bi400585h | *Biochemistry* 2013, 52, 5256−5264

actin is not through specific actin-binding sites. F-actin bundles formed by the "wrapping" model are dense and may also be flexible, which can explain the elasticity of rootlets which is needed in response to the wide range of mechanical stresses imposed on stereocilia pivots during sound stimulation.[34] It would be of great interest to directly measure the rigidity and stiffness of TRIOBP-4 formed bundles.

Though the R2 motif exhibited some F-actin binding/bundling activities and formed thin bundles (Figures 2−5, Supplemental Figures S1−3), the F-actin dissociation constant (K_d) of the GFP-$T4_{599-980}$ is significantly increased in a longer fragment having additional amino acids (GFP-$T4_{\Delta 357-605}$) and a shorter fragment with deletion of GFP (i.e., $T4_{599-980}$ protein), suggesting that the actin-binding activity of R2 motif is not correlated with the size of the R2-containing fragments, and its biochemical property or structure may be easily affected by addition or deletion of other amino acids nearby. Moreover, when overexpressed in cells, in contrast to the colocalization of R1 motif with F-actin including in filopodia where parallel F-actin bundles are present, the R2 motif did not localize to any cellular actin cytoskeleton structures (Figure 6), further supporting the hypothesis that the *in vitro* binding of R2 to F-actin is due to nonspecific interaction.

The mobility of TRIOBP-4 fragments on SDS-PAGE is not consistent with their expected molecular weights (Figure 1D). We think this is caused by the high content proline content (>10% of total amino acids) present in all the TRIOBP-4 fragments tested. As the structure of proline is not compatible with the necessary phi and psi backbone torsional angles of the α helix, thus it would inhibit the α-helical structures that are typically induced by SDS in its denatured proteins.

In addition to expression in inner ear hair cells, TRIOBP-4 is also detected in the retina, testis, and kidney, but the function of TRIOBP-4 in these other tissues is not yet known.[2,3] Our RT-PCR results indicate a broader expression of TRIOBP-4 in several human cancer cell lines (Figure 6A). Intrinsically disordered proteins have been implicated in cell division and cancer-associated diseases.[35−37] Thus, our studies examining the actin bundling mechanism by TRIOBP-4 will provide useful information not only for understanding the molecular basis of deafness caused by mutation of TRIOBP, but also its role in resilient cytoskeleton structures in other tissues and pathological processes.

■ ASSOCIATED CONTENT

Supporting Information

Figures and figure legends. This material is available free of charge via the Internet at http://pubs.acs.org.

■ AUTHOR INFORMATION

Corresponding Author

*(T.S.) Address: Department of Physics and Astronomy, Wayne State University, 666 W. Hancock Street, Suite 287, Detroit, MI 48201. Phone: 313-577-2970. E-mail: ee4243@wayne.edu. (S.K.) Department of Otolaryngology - Head and Neck Surgery, Kyoto University Graduate School of Medicine, 54 Shogoin Kawaharacho, Sakyo-ku, Kyoto 606-8507, Japan. Phone: +81-75-751-3346. E-mail: kitajiri@ent.kuhp.kyoto-u.ac.jp.

Funding

This work was supported by K99/R00 Career Grant (R00HL089350) and start-up from Department of Physics and Astronomy, Wayne State University, to T.S.

Notes

The authors declare no competing financial interests.

■ ACKNOWLEDGMENTS

We acknowledge the professional support of the Microscope, Imaging and Cytometry Resources Core (MICR) of Wayne State University School of Medicine and the Laboratory of Analytical Electron Microscopy (LAEM), Department of Chemistry, Wayne State University. We thank Dr. Dorothy Sorenson and Dr. Kristen Verhey (University of Michigan) for use of their glow discharger. We thank Dr. James R. Sellers (NHLBI, NIH, Bethesda, MD), Dr. James R. Bartles (Northwestern University, Chicago, IL), and Dr. Thomas B. Friedman (NIDCD, NIH, Rockville, MD) for the discussion and comments.

■ ABBREVIATIONS

TRIOBP-4: TRIOBP isoform 4; R1 motif: the first repeated motif of TRIOBP-4/-5; R2 motif: the second repeated motif of TRIOBP-4/-5; TEM: transmission electron microscope; GFP-T4: GFP-TRIOBP-4

■ REFERENCES

(1) Kitajiri, S., Sakamoto, T., Belyantseva, I. A., Goodyear, R. J., Stepanyan, R., Fujiwara, I., Bird, J. E., Riazuddin, S., Ahmed, Z. M., Hinshaw, J. E., Sellers, J., Bartles, J. R., Hammer, J. A., 3rd, Richardson, G. P., Griffith, A. J., Frolenkov, G. I., and Friedman, T. B. (2010) Actin-bundling protein TRIOBP forms resilient rootlets of hair cell stereocilia essential for hearing. *Cell 141*, 786−798.

(2) Riazuddin, S., Khan, S. N., Ahmed, Z. M., Ghosh, M., Caution, K., Nazli, S., Kabra, M., Zafar, A. U., Chen, K., Naz, S., Antonellis, A., Pavan, W. J., Green, E. D., Wilcox, E. R., Friedman, P. L., Morell, R. J., and Friedman, T. B. (2006) Mutations in TRIOBP, which encodes a putative cytoskeletal-organizing protein, are associated with nonsyndromic recessive deafness. *Am. J. Hum. Genet. 78*, 137−143.

(3) Shahin, H., Walsh, T., Sobe, T., Abu Sa'ed, J., Abu Rayan, A., Lynch, E. D., Lee, M. K., Avraham, K. B., King, M. C., and Kanaan, M. (2006) Mutations in a novel isoform of TRIOBP that encodes a filamentous-actin binding protein are responsible for DFNB28 recessive nonsyndromic hearing loss. *Am. J. Hum. Genet. 78*, 144−152.

(4) Seipel, K., O'Brien, S. P., Iannotti, E., Medley, Q. G., and Streuli, M. (2001) Tara, a novel F-actin binding protein, associates with the Trio guanine nucleotide exchange factor and regulates actin cytoskeletal organization. *J. Cell Sci. 114*, 389−399.

(5) Yano, T., Yamazaki, Y., Adachi, M., Okawa, K., Fort, P., Uji, M., and Tsukita, S. (2011) Tara up-regulates E-cadherin transcription by binding to the Trio RhoGEF and inhibiting Rac signaling. *J. Cell Biol. 193*, 319−332.

(6) Zheng, L., Sekerkova, G., Vranich, K., Tilney, L. G., Mugnaini, E., and Bartles, J. R. (2000) The deaf jerker mouse has a mutation in the gene encoding the espin actin-bundling proteins of hair cell stereocilia and lacks espins. *Cell 102*, 377−385.

(7) Sekerkova, G., Zheng, L., Loomis, P. A., Changyaleket, B., Whitlon, D. S., Mugnaini, E., and Bartles, J. R. (2004) Espins are multifunctional actin cytoskeletal regulatory proteins in the microvilli of chemosensory and mechanosensory cells. *J. Neurosci. Official J. Soc. Neurosci. 24*, 5445−5456.

(8) Drenckhahn, D., Engel, K., Hofer, D., Merte, C., Tilney, L., and Tilney, M. (1991) Three different actin filament assemblies occur in every hair cell: each contains a specific actin crosslinking protein. *J. Cell Biol. 112*, 641−651.

(9) Zine, A., Hafidi, A., and Romand, R. (1995) Fimbrin expression in the developing rat cochlea. *Hear Res. 87*, 165−169.
(10) Daudet, N., and Lebart, M. C. (2002) Transient expression of the t-isoform of plastins/fimbrin in the stereocilia of developing auditory hair cells. *Cell Motil. Cytoskeleton 53*, 326−336.
(11) Shin, J. B., Longo-Guess, C. M., Gagnon, L. H., Saylor, K. W., Dumont, R. A., Spinelli, K. J., Pagana, J. M., Wilmarth, P. A., David, L. L., Gillespie, P. G., and Johnson, K. R. (2010) The R109H variant of fascin-2, a developmentally regulated actin crosslinker in hair-cell stereocilia, underlies early-onset hearing loss of DBA/2J mice. *J. Neurosci. Official J. Soc. Neurosci. 30*, 9683−9694.
(12) Chou, S. W., Hwang, P., Gomez, G., Fernando, C. A., West, M. C., Pollock, L. M., Lin-Jones, J., Burnside, B., and McDermott, B. M., Jr. (2011) Fascin 2b is a component of stereocilia that lengthens actin-based protrusions. *PLoS One 6*, e14807.
(13) Flock, A., and Cheung, H. C. (1977) Actin filaments in sensory hairs of inner ear receptor cells. *J. Cell Biol. 75*, 339−343.
(14) Yang, Y., Kovacs, M., Sakamoto, T., Zhang, F., Kiehart, D. P., and Sellers, J. R. (2006) Dimerized Drosophila myosin VIIa: a processive motor. *Proc. Natl. Acad. Sci. U. S. A. 103*, 5746−5751.
(15) Spudich, J. A., and Watt, S. (1971) The regulation of rabbit skeletal muscle contraction. I. Biochemical studies of the interaction of the tropomyosin-troponin complex with actin and the proteolytic fragments of myosin. *J. Biol. Chem. 246*, 4866−4871.
(16) Veigel, C., Bartoo, M. L., White, D. C., Sparrow, J. C., and Molloy, J. E. (1998) The stiffness of rabbit skeletal actomyosin cross-bridges determined with an optical tweezers transducer. *Biophys. J. 75*, 1424−1438.
(17) Sakamoto, T., Wang, F., Schmitz, S., Xu, Y., Xu, Q., Molloy, J. E., Veigel, C., and Sellers, J. R. (2003) Neck length and processivity of myosin V. *J. Biol. Chem. 278*, 29201−29207.
(18) Thirumurugan, K., Sakamoto, T., Hammer, J. A., 3rd, Sellers, J. R., and Knight, P. J. (2006) The cargo-binding domain regulates structure and activity of myosin 5. *Nature 442*, 212−215.
(19) Kelley, L. A., and Sternberg, M. J. (2009) Protein structure prediction on the Web: a case study using the Phyre server. *Nat. Protoc. 4*, 363−371.
(20) Dosztanyi, Z., Csizmok, V., Tompa, P., and Simon, I. (2005) IUPred: web server for the prediction of intrinsically unstructured regions of proteins based on estimated energy content. *Bioinformatics 21*, 3433−3434.
(21) Prilusky, J., Felder, C. E., Zeev-Ben-Mordehai, T., Rydberg, E. H., Man, O., Beckmann, J. S., Silman, I., and Sussman, J. L. (2005) FoldIndex: a simple tool to predict whether a given protein sequence is intrinsically unfolded. *Bioinformatics 21*, 3435−3438.
(22) Romero, P., Obradovic, Z., Li, X., Garner, E. C., Brown, C. J., and Dunker, A. K. (2001) Sequence complexity of disordered protein. *Proteins 42*, 38−48.
(23) Matsudaira, P. (1991) Modular organization of actin cross-linking proteins. *Trends Biochem. Sci. 16*, 87−92.
(24) Stokes, D. L., and DeRosier, D. J. (1991) Growth conditions control the size and order of actin bundles in vitro. *Biophys. J. 59*, 456−465.
(25) Tilney, L. G., Tilney, M. S., and Guild, G. M. (1995) F actin bundles in Drosophila bristles. I. Two filament cross-links are involved in bundling. *J. Cell Biol. 130*, 629−638.
(26) Furukawa, R., and Fechheimer, M. (1997) The structure, function, and assembly of actin filament bundles. *Int. Rev. Cytol. 175*, 29−90.
(27) Puius, Y. A., Mahoney, N. M., and Almo, S. C. (1998) The modular structure of actin-regulatory proteins. *Curr. Opin. Cell Biol. 10*, 23−34.
(28) Goldsmith, S. C., Pokala, N., Shen, W., Fedorov, A. A., Matsudaira, P., and Almo, S. C. (1997) The structure of an actin-crosslinking domain from human fimbrin. *Nature Struct. Biol. 4*, 708−712.
(29) Bartles, J. R., Zheng, L., Li, A., Wierda, A., and Chen, B. (1998) Small espin: a third actin-bundling protein and potential forked protein ortholog in brush border microvilli. *J. Cell Biol. 143*, 107−119.
(30) Yamashiro-Matsumura, S., and Matsumura, F. (1985) Purification and characterization of an F-actin-bundling 55-kilodalton protein from HeLa cells. *J. Biol. Chem. 260*, 5087−5097.
(31) Jansen, S., Collins, A., Yang, C., Rebowski, G., Svitkina, T., and Dominguez, R. (2011) Mechanism of actin filament bundling by fascin. *J. Biol. Chem. 286*, 30087−30096.
(32) Yan, Y., Winograd, E., Viel, A., Cronin, T., Harrison, S. C., and Branton, D. (1993) Crystal structure of the repetitive segments of spectrin. *Science 262*, 2027−2030.
(33) Pascual, J., Castresana, J., and Saraste, M. (1997) Evolution of the spectrin repeat. *BioEssays 19*, 811−817.
(34) Richardson, G. P., de Monvel, J. B., and Petit, C. (2011) How the genetics of deafness illuminates auditory physiology. *Annu. Rev. Physiol. 73*, 311−334.
(35) Fink, A. L. (2005) Natively unfolded proteins. *Curr. Opin. Struct. Biol. 15*, 35−41.
(36) Uversky, V. N., Oldfield, C. J., and Dunker, A. K. (2008) Intrinsically disordered proteins in human diseases: introducing the D2 concept. *Annu. Rev. Biophys. 37*, 215−246.
(37) Galea, C. A., Wang, Y., Sivakolundu, S. G., and Kriwacki, R. W. (2008) Regulation of cell division by intrinsically unstructured proteins: intrinsic flexibility, modularity, and signaling conduits. *Biochemistry 47*, 7598−7609.